Int. J. Electrochem. Sci., 6 **(2011)** 2746 - 2757

International Journal of
ELECTROCHEMICAL
SCIENCE
www.electrochemsci.org

Solution Conductivity Influence on Pitting Corrosion Studies by SVET

R. Zlatev, B. Valdez, M. Stoytcheva[*], *R. Ramos, S. Kiyota*

Engineering Institute of UABC, Blvd. Benito Juárez s/n, Mexicali 21280, B. C., México
[*]E-mail: margarita@iing.mxl.uabc.mx

Received: 4 May 2011 / *Accepted:* 30 May 2011 / *Published:* 1 July 2011

The controversial statements about the solution conductivity changes occurring above the pits appeared on corroded Al alloy surface were verified. Original local conductometric measuring technique was employed together with SVET to evaluate the solution conductivity influence on the SVET results, completely dependent on the solution conductivity ($IR_{solution}$ ohmic drop). Bare and chromated AA 7075-T6 aerospace aluminum alloy specimens were employed in 5 % NaCl solutions for the conductometric/SVET measurements. Artificial "pits" (Pt spots) with known dimensions were used for the SVET measuring instrument calibration. Solution conductivity variations of about 4.8 % above the non-chromated specimens' surfaces were registered at a distance of 30 µm 5 minutes after the specimens' immersion, against less than 1% changes above the chromated specimens at same conditions. A special noise reduction technique was applied allowing distinguishing of the small changes of the SVET signal caused by the conductivity influence.

Keywords: AA 7075 alloy, pitting corrosion, chromate conversion coating, SVET, local conductivity

1. INTRODUCTION

Localized measuring techniques such as Scanning Vibrating Electrode Technique (SVET) [1-3] and Scanning Reference Electrode Technique (SRET) [4, 5] are powerful tools for pitting corrosion studies. SVET, being a further improvement of SRET provides higher sensitivity due to the conversion of the measured potential gradient into AC signal achieved by probe vibrating. The lock-in amplifier application allows recovering of the very low SVET signals from the extremely noisy environment at more than 60 dB signal to noise ratio (S/N). As a result, amplitudes as low as 5 µV are able to be measured by SVET allowing distinguishing of very small corroded zones, while the minimal potential gradients measurable by SRET are reported to be about 200 µV [6, 7].

The localized techniques allow the determination of the ionic currents distribution flowing between the anodic and the cathodic zones of the corroded surface through the solution, and the corrosion rate determination as well [8]. The ionic currents are evaluated by measurement of the potential gradients appearing as ohmic drops: $U = IR$ resulting from the currents flowing through the test solution. Since U depends on the solution resistance $R = 1/\sigma$ (where σ is the solution conductivity) the local solution conductivity appears to be an important parameter determining the SVET results. Oltra [9] stated that the ohmic drop existence stabilizes the localized corrosion processes becoming part of the electrochemical polarization of the system in terms of electrochemical kinetics.

The local conductivity may differ from the bulk one because of: i) the metal dissolution caused by the corrosion process; ii) insoluble corrosion products formation with the participation of ions from the nearest metal surface environment as stated by Vuillemin *et al.* [10] reporting dynamic local changes in surface composition due to precipitation of dissolved species.

The localized corrosion processes can be characterized more completely employing simultaneously several independent local measuring techniques [9]. Ogle *et al*. [11] reported a combination of local pH and current density measurements applied to galvanized steel cut edge corrosion studies. Park and Böhni [12] combined pH measurement with polarization curves registration applied to local corrosion sites containing MnS inclusions. Vuillemin *et al*. [10] reported a combination of SVET, AFM and SAM (Scanning Auger Microscopy) applied to pitting corrosion of a MnS inclusion on 316L stainless steel, employing aggressive solution injection (NaCl, H_2SO_4 or HCl).

As established by Oltra [9], significant changes in solution chemistry may occur very close to the corroded surface, so that the conductivity may be unknown and some of the currents can be controlled by diffusion as well because of the decreased ion concentrations.

On the other hand, Deshpande [13] stated that the local solution conductivity variations are marginal (less than 0.4%) confirming that there was no difference between the bulk conductivity and those close to the galvanic couple. Probably both controversial statements can be true but related to different conditions such as corroded alloy and test solution composition, protection coatings existence and composition etc. No data were published till now proving or denying some of the mentioned controversial statements.

The objectives of the present work is real time local conductivity monitoring of the NaCl test solution above the corroded bare and chromated AA 7075 T6 aluminum alloy in 5% NaCl test solution, at a distance of 30 μm from artificial pits simultaneously with SVET measurements to evaluate the conductivity changes influence on the SVET results.

2. EXPERIMENTAL

2.1. Artificial microcells (pits) preparation

An artificial microcell imitating anodic and cathodic pits zones was elaborated and used for the SVET instrument calibration. It consisted of two Pt wires 0.1 mm in diameter placed in acrylic resin

support at a distance of 25 μm between them, connected to a homemade low current galvanostat. The acrylic cylinder was polished using finally 1 μm alumina to appear two Pt spots on it.

Another artificial cell was prepared by the same way but replacing one of the Pt wires by AA 7075 T6 one, 0.1 mm in diameter serving as anode zone connected to the galvanostat. The aluminum alloy wire was prepared by rolling of 5 mm thick bar down to 1 mm followed by slow mechanical extension down to about 0.1 mm at increased temperature achieved by electric current passing through the extended wire.

2.2. Specimens Preparation

Bare AA 7075 T6 specimens measured 1x1 cm were capsulated in acrylic resin and then polished with abrasive sand paper up to #1500 and finally by 1 μm alumina. The half of the capsulated specimens were chromated applying industrial alodining process yielding coatings composition: $Cr(OH)_2HCrO_4$ and $Cr_2O_3.1.2H_20$ (48 to 80 %); Al_2O_3, AlF_3, AlOF, AlOOH (15 to 30%).

The pits occurrence on the bare and chromated specimens' surface was provoked by immersion into the testing electrolyte followed by SVET/conductivity measurements. For comparison specimens kept in saline chamber according to the ASTM 117 condition were employed as well.

2.3. Testing Electrolyte

A relatively high salt concentration 5% (0.86mol dm^{-3}) of NaCl solutions with a conductivity of 7.01 Sm^{-1} at 20°C was chosen to obtain a sufficiently high signal for the local conductivity avoiding the influence of the conductometric electrodes (probe tips) small size. Deionized water produced by Milli Q reverse osmosis installation (Millipore, USA) was employed for the testing solutions preparation.

2.4. SVET - Conductometric Equipment

Homemade equipment was employed for the simultaneous SVET and conductivity measurements with the application of two vibrating probes setup. One of the probes was connected to the amplifier input applied for both, SVET potential gradient ($IR_{solution}$ ohmic drop) and conductivity measurements as well.

Pulses of AC sine wave voltage with frequency of 60 Hz, duration of 33.3 ms (two periods of 60 Hz) and amplitude of 100 mV p-p was applied to the second probe at the end of every step of the surface scan performed by precise X-Y linear stages. Voltage driven lens focusing mechanism commonly used in the CD/DVD computer drives was employed for Z direction conductometry/SVET combined probe positioning within +/-1.5 mm and for its vibration with amplitude of 10 μm at a distance of 30 μm from the specimen controlled by a microscope.

A NI USB 6009 Data Acquisition System coupled with especially developed NI Lab View 8.0 based software were used for SVET and conductivity signals data acquisition and for the X-Y stage driving with a step of 0.5 μm.

2.4. SVET noise suppression technique

The noise spectrum analysis of the SVET signal showed that the main noise frequency is the power line one F = 60 Hz (or 50 Hz). For its suppression the specific approach developed by the authors earlier [14] was applied. For this purpose the frequency of the SVET tip vibration was chosen to be F/2 (obtained by dividing the power line frequency by 2) allowing the entire cycle of the tip movement (neutral – down – neutral – up - neutral) to happen within two full power line periods. Digital integration of the SVET signal was applied for every of these two periods and finally, the two integral products were subtracted yielding the SVET measurement value. Since the noise coming from the power line is the same for every one of the two integration periods (coinciding completely with the SVET tip movement cycle) the integral products subtraction eliminates completely the power line noise reducing also the white (rose) noise level. Thus, a total noise suppression of 61 dB (about 1000 times) was achieved without lock-in amplifier application.

3. RESULTS AND DISCUSSION

3.1. SVET equipment calibration

The voltage gradient ($IR_{solution}$ ohmic drop) measured by SVET can be converted into ion current density applying the following equation proposed by Ogle *et al*. [12]:

$$j = \sigma\,(\Delta E/A) \qquad (1)$$

where: j is the current density; σ is the specific conductivity of the electrolyte solution; ΔE is the potential gradient across the vibration amplitude; A is the vibration amplitude.

Since σ and A are constants, this equation can be presented simpler as: $j = K\,\Delta E$ assuming the temperature to be constant (since σ is temperature dependent). Thus, the aim of the SVET calibration is the experimental determination of the coefficient K. The acrylic cell with two artificial "pits" - Pt disc electrodes imitating the anodic and cathodic pits zones described above was employed for this purpose. Known constant currents I in the range from 0.2 to 10 μA were imposed between them from a galvanostat able to maintain small currents and the Pt micro-disc anode was scanned by the SVET vibrating probe at a constant distance of 30 μm. The maximal potential gradient ΔE, measured at the center of the Pt disc was plotted against the imposed constant current I, shown in Fig. 1 having plot characteristics: b[0] = 1.831; b[1] = 57.297 and $r^2 = 0.998$

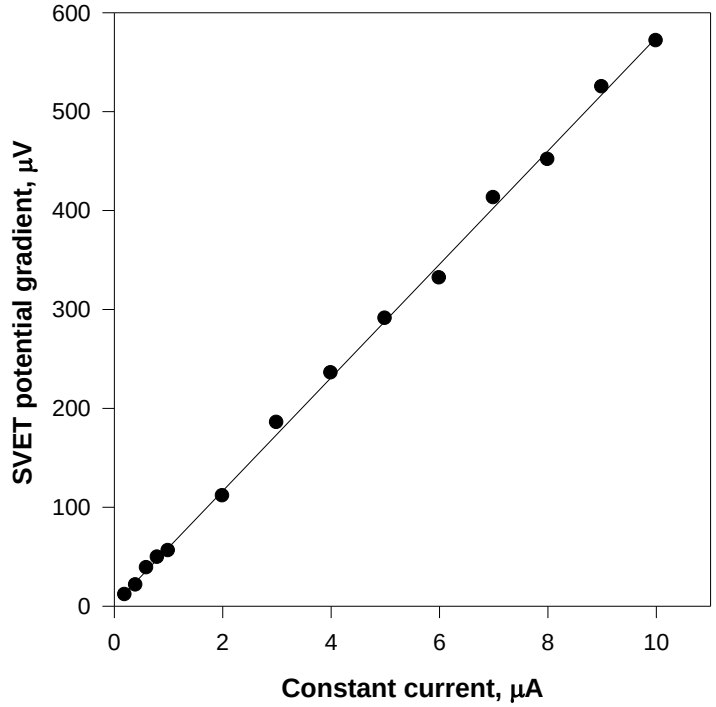

Figure 1. SVET signal calibration plot obtained in 5% NaCl test solution and artificial pit employment.

Taking into account the Pt electrode surface of 7.85 10^{-9} m^2 and converting the applied constant current in current density, the coefficient *K* calculated as slope of the curve was found to be 1.274 10^2 A V^{-1} m^{-2}.

3.3. Conductometric equipment calibration

NaCl water solutions with known concentrations from 10 to 60 g L^{-1} (1 to 6 %) were employed for calibration plot building in coordinates: conductivity AC current – NaCl solution concentration presented in Fig. 2 having the following characteristics: b[0]= -1.086; b[1] = 3.151; r^2 = 0.988.

The concentration can be easily converted in conductivity measured in (S m^{-1}) by replacing the concentration values with the corresponding conductivity ones measured by a commercial conductometer or taken from a table. In this paper however all the measured conductivity data are presented using their corresponding concentrations in accordance to Figure 2.

When the conductivity measurements were carried out at a temperature different from the calibration one, temperature compensation was made applying the following equation:

$$\sigma_t = \sigma_{tcal}[1 + \alpha(t\text{-}t_{cal})] \quad (2)$$

where: σ_t is the solution conductivity at temperature *t*; σ_{tcal} is the solution conductivity at the temperature of the calibration; α = 2%/^{o}C for NaCl solutions.

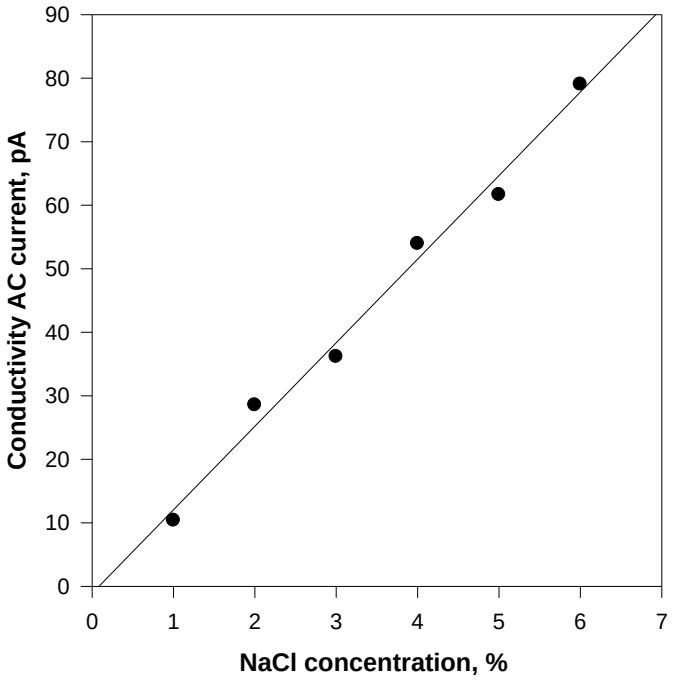

Figure 2. Conductivity calibration plot, obtained by microprobes electrodes in 5% NaCl test solution.

3.2. Precise pit's size determination by AFM application

Pits, having equivalent diameters about 100 μm similar to the diameters of the artificial ones were employed in the real specimens experiment, and also because of the technical difficulties in preparation of smaller artificial ones. The pit sizes were determined by the application of optical microscope and AFM as well. A partial pit's AFM image is shown in Fig. 3.

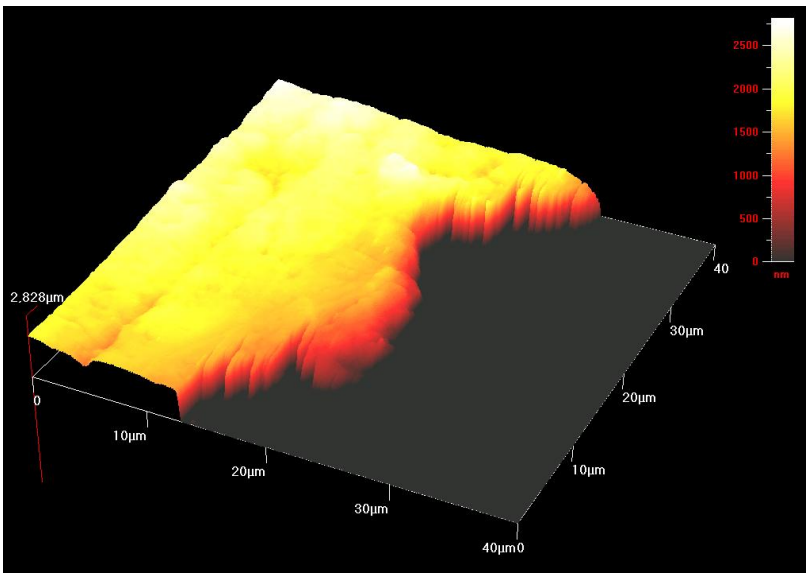

Figure 3. Partial AFM image of a pit (black zone) on a chromated (yellow zone) AA 7075 T6 alloy surface.

3.4. Bare specimens testing: simultaneous ion current density and conductivity measurement

The bare metals exhibited dynamic zones of anodic activity, reflecting sites of localized corrosion when immersed in test NaCl solution. The pits appeared almost immediately, causing significant currents flowing registered during the first SVET scans followed by rapid diminution due to metal passivation on a time scale of tens of minutes. Family of SVET profiles registered by multiple one dimension scan (X axe only, keeping Y = 0) of same pit area every 5 minutes during 20 minutes are shown in Fig. 4. The anodic current decrease with the time can be explained with the passivation, while the cathodic sites are affected by corrosion products precipitation provoking the same result.

The conductivity profile registered simultaneously with the SVET after the specimen immersion is shown in Fig. 5. Maximal deviation of 4.8% was observed at 30 μm above the anodic zones 5 minutes after the specimens' immersion probably due to the metal dissolution, while above the cathodic zones no conductivity change occurred. Obviously, the precipitation appeared above the cathodic site is not capable to decrease the local solution concentration at the interface with the metal since the Na-aluminates are soluble.

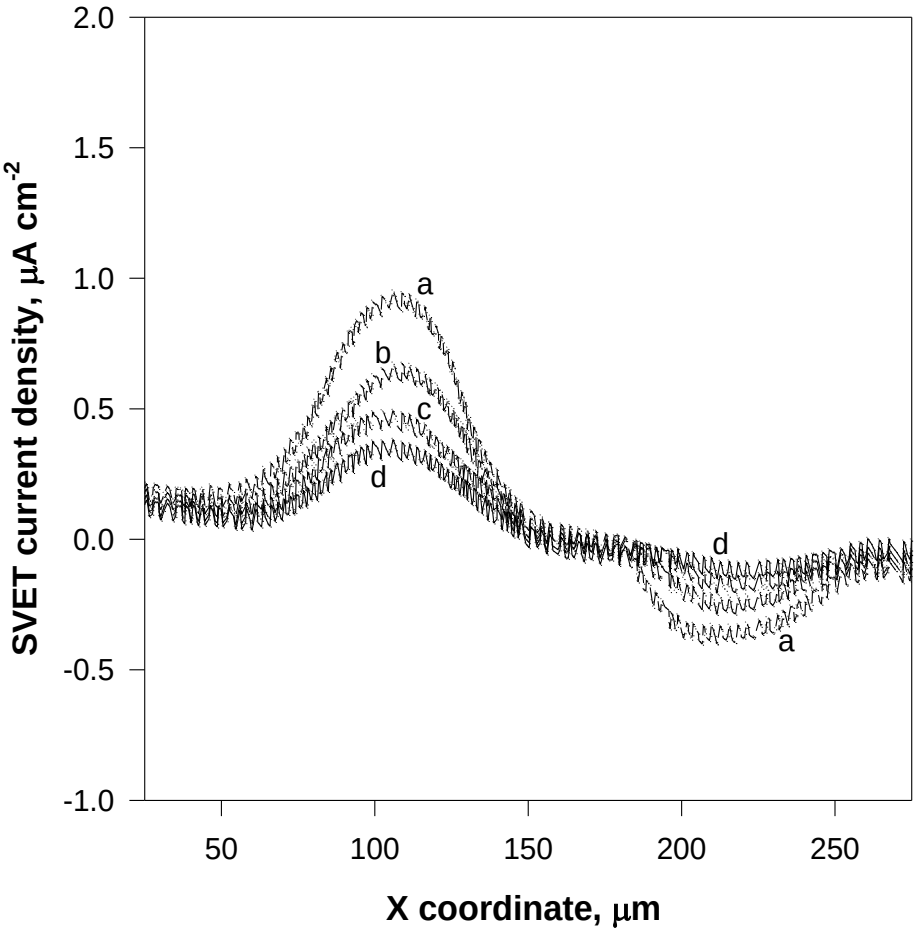

Figure 4. SVET current density/X coordinate plot above the pit located on bare AA 7075 surface. Curves from **a** to **d** were registered: 5; 10; 15 and 20 minutes respectively after the specimen's immersion into 5% NaCl test solution.

In general, a precipitation strongly depending on the solution and the corroded metal composition can appear provoked by the pH augmentation due to the following cathodic reaction:

$$O_2 + 2H_2O + 4e^- = 4OH^- \quad [2]$$

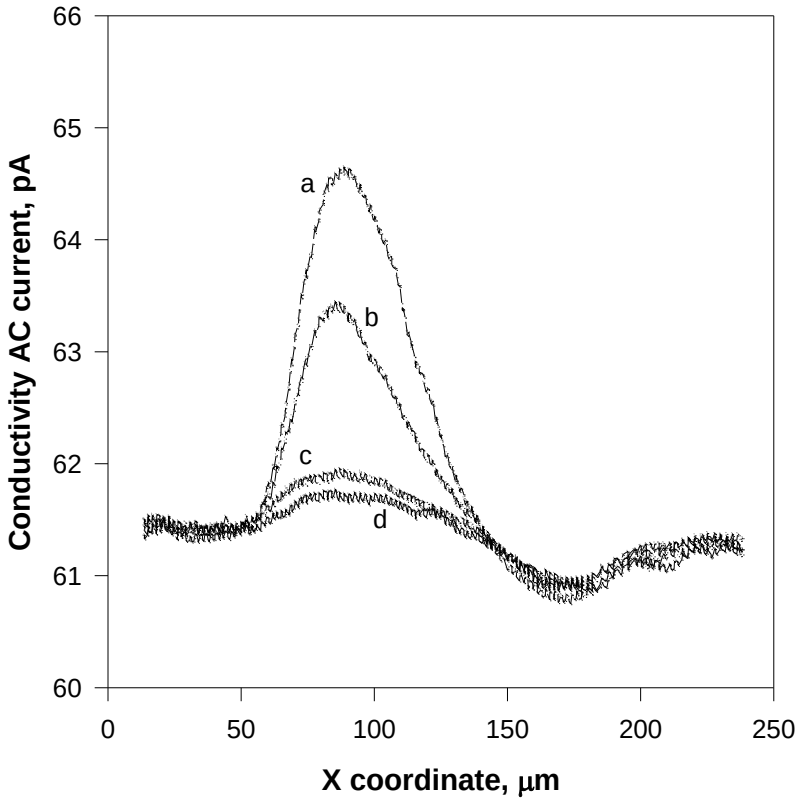

Figure 5. Local conductivity/X coordinate plot above the pit characterized by SVET in Fig. 4. Curves from **a** to **d**: 5; 10; 15 and 20 minutes respectively after the specimen's immersion into 5% NaCl test solution.

The values obtained for the maximal local conductivity variations above the bare metal surface of 4.8% are much higher than those (0.4%), reported by Deshpande [13]. On the other hand *"significant changes in solution chemistry"* stated by Oltra [9] was not registered. The observed conductivity increase faded to its initial (bulk) value due to the surface passivation becaming almost undistinguishable from the noise 15 minutes after the immersion.

3.5. Chromated specimens testing: simultaneous ion current density and conductivity measurements

Specimens chromated by industrial alodining process application including 60 s chromatizing stage were employed. Although the mechanisms of the inhibition of the Al alloys corrosion by chromate conversion coatings remains still unclear, it is assumed that Cr^{6+} inhibits the cathodic reactions (primarily oxygen reduction) on the alloy active sites [15, 16] blocking thus the consumption

of the electrons generated from the metal oxidation step at the anodic sites. Several redox reactions may occur such as: direct oxidation of the metal substrates provoked by the oxidizing power of CrO_4^{2-} or Cr^{6+}; Cr^{6+} reduction to Cr^{3+} with composite oxide/hydroxide adherent films formation having a general composition: xAl_2O_3/yCr_2O_3 or $xAl(OH)_3/yCr(OH)_3$, where x and y are variable depending on conditions [17]. On the other hand the negative charge of CrO_4^{2-} and $Cr_2O_7^{2-}$ facilitates Cr^{6+} migration to anodic sites where passivation processes may occur. As a result the chromate coatings provide regenerating properties protecting mainly the damaged areas by pits sealing as stated by Adrian and Bittner [18]. The potentiodynamic Tafel plots presented in Fig. 6 registered for a single pit 5 and 20 minutes respectively after the specimen immersion into the NaCl test solution showed time dependant anodic current diminition proving the pit sealing. The anodic current diminution within 15 minutes was found to be about 6 times and the pitting potential remains almost unchanged during the pit sealing. After the pits sealing, negligible corrosion activity and hence local solution conductivity changes could be expected above the sealed pit's zone.

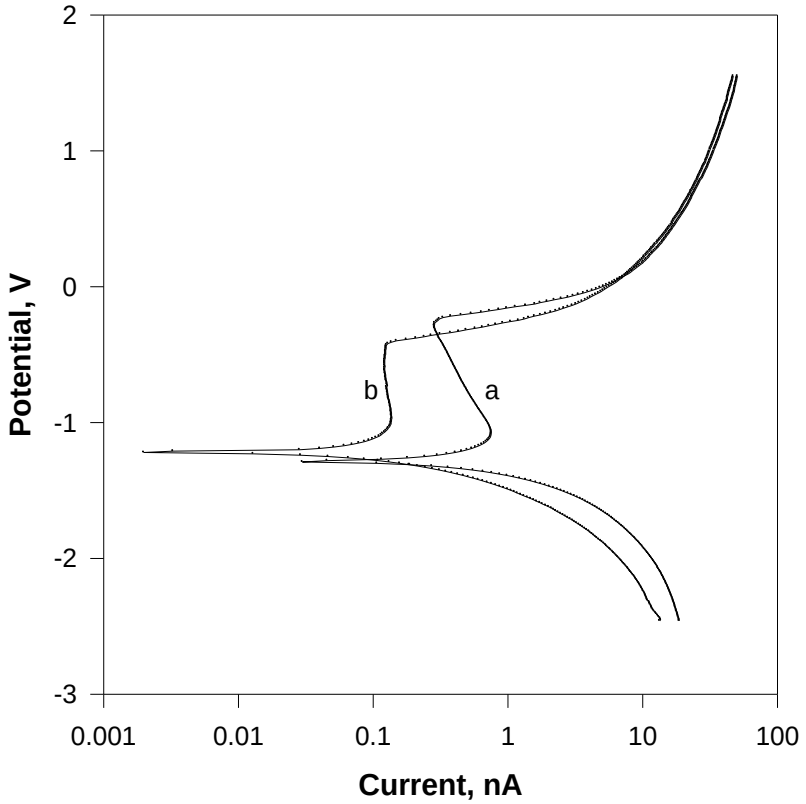

Figure 6. Fig. 6. Tafel plots of a pit on chromated (60 s) AA 7075-T6 aluminum alloy. The curves **a** and **b** were registered 5 and 20 minutes after the specimen's immersion into 5% NaCl test solution.

The SVET measurements showed decreased maximal anodic current amplitudes compared with the bare samples results. Family of SVET plots are presented in Fig. 7 measured during 20 minutes after specimen's immersion in 5 minutes intervals. The pit appearing was initiated by scratching the chromated surface in order to obtain comparable conditions with bare samples.

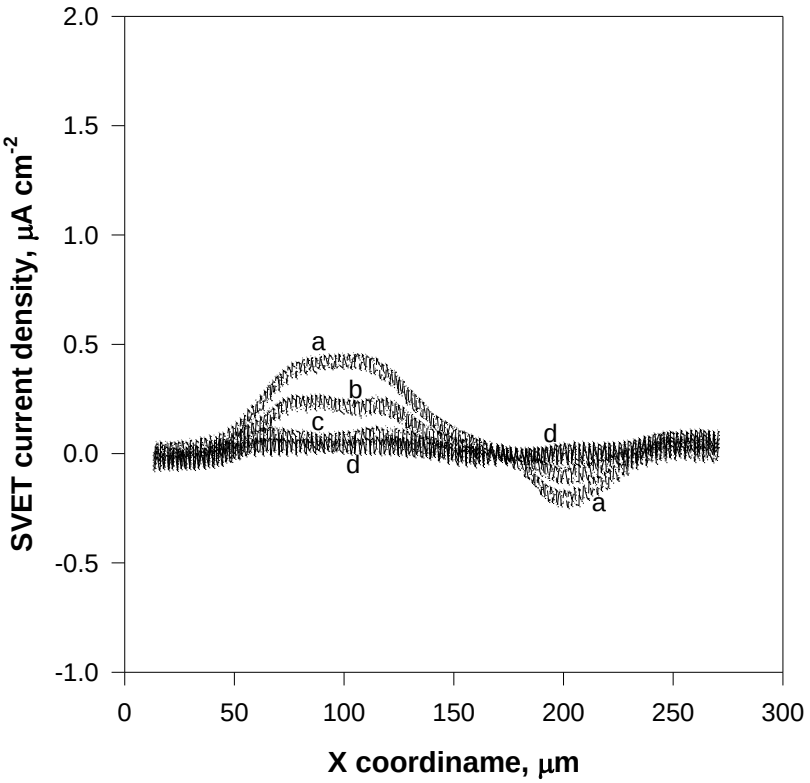

Figure 7. SVET current density/X coordinate plots above a pit on chromated AA 7075 T6 alloy. Curves from **a** to **d** were registered: 5; 10; 15 and 20 minutes respectively after the specimen's immersion into 5% NaCl test solution.

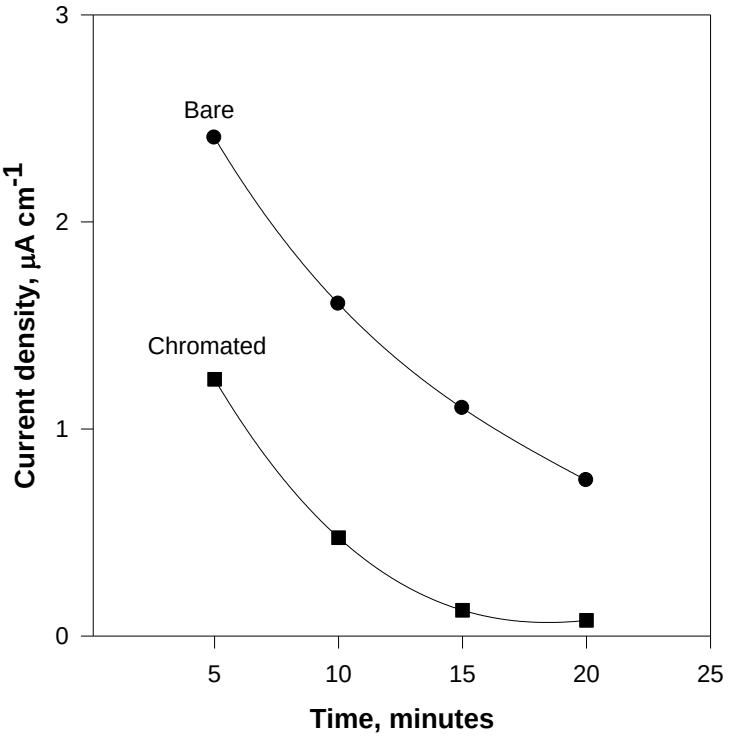

Figure 8. Maximal current density/time profiles comparison of bare and chromated specimens in 5% NaCl test solution. Data derived from the Figures 4 and 7.

The maximal ion current density measured by SVET 5 minutes after the chromated specimen immersion into the test solution were found to be about two times lower compared with the bare specimens, while 15 minutes later the difference was already about 10 times, as seen from Fig. 8, where the current density/time profile for chromated AA 7075 specimens is presented. The diminished corrosion activity in this case is due obviously to the self regenerating properties of the chromate coatings.

The local conductivity results above the chromated AA 7075 specimen's are also affected by the pits sealing which prevents significant solution conductivity variations. The local conductivity plots measured 5 and 10 minutes after the specimen's immersion are shown in Fig. 9. After the 10th minute from the specimen's immersion (see curves c and d in Fig. 9) the test solution conductivity variations are already too small, not distinguishable from the noise.

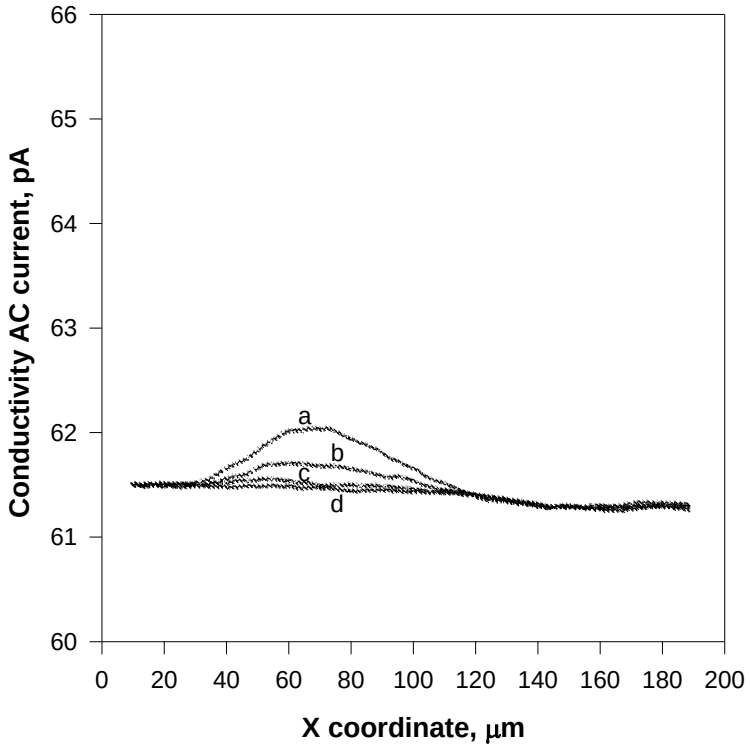

Figure 9. Local conductivity/X coordinate plot above the pit characterized by SVET presented in Fig. 4. Curves from a to d: 5; 10; 15 and 20 minutes respectively after the specimen's immersion into 5% NaCl test solution.

4. CONCLUSIONS

The controversial statements of about the local conductivity variations of test solution during the corrosion process and their influence on the SVET results were verified combining the SVET with

local conductivity measurements. A special noise suppression technique was applied allowing to detect small SVET signal changes due to the local test solution conductivity variations.

It was found that the maximal conductivity changes are less than 1% occuring above the chromated AA 7075-T6 specimens, 5 minutes after the specimen's immersion, measured at a distance of 30 μm from the corroded metal surface. The conductivity changes above the bare AA 7075-T6 specimens however are considerably higher: 4.8% maximal value measured at the same conditions.

The obtained results lead to the conclusion that the conductivity changes depend on the type of the corroded metal surface and its conditions (coated or bare), explaining thus the controversial statements mentioned above.

References

1. L. Jaffe and R. Nuccitelli, *J. Cell Biology*, 63 (1974) 614
2. H. S. Isaacs in R. Staehle, B. Brown, J. Kruger and A. Agarwal (Eds), *Localized Corrosion*, NACE-3, NACE, Houston, TX, USA, (1974) p. 158.
3. H. S. Isaacs, *J. Electrochem. Soc*., 138 (1991) 722
4. H. S. Isaacs and Y. Ishikawa, *J. Electrochem. Soc*., 132 (1985) 1288
5. S. Fujimoto and T. Shibata, *Denki Kagaku*, 64 (1996) 967
6. E. Gileadi, E. Kirowa-Eisner and J. Penciner, *Interfacial Electrochemistry-an experimental approach*, Addison-Wesley Publishing Co., Inc., Reading, MA, USA, (1975) 216
7. K. R. Trethewey, D. A. Sargeant, D. J. Marsh and A. A. Tamimi, *Corrosion Science*, 35 (1993) 127
8. C. Wagner, *J. Electrochem. Soc*., 98 (1951) 116
9. R. Oltra in: R. Oltra, V. Maurice, R. Akid and P. Marcus (Eds.), *Local probe techniques for corrosion research*, European Federation of Corrosion Publications, number 45, CRC Press, Woodhead Publishing and Maney Publishing, Cambridge England, (2007)
10. B. Vuillemin, X. Philippe, R. Oltra, V. Vignal, L. Coudreuse, L. C. Dufour and E. Finot, *Corrosion Science*, 45 (2003) 1143
11. K. Ogle, V. Baudu, L. Garrigues and X. Philippe, *J. Electrochem. Soc*., 147 (2000) 3654
12. J. O. Park and H. Böhni, *Electrochem. Solid-State Lett*., 3 (2000) 416
13. K. B. Deshpande, *Corrosion Science*, 52 (2010), 2819
14. R. Ramos, R. Zlatev, M. Stoytcheva, B. Valdez, S. Flores, and A. M. Herrera, *ECS Transactions*, 29 (1) (2010) 33
15. He Jie, V. J. Gelling, D. E. Tallman and G. P. Bierwagen, *J. Electrochem. Soc*., 147 (2000) 3661
16. N. N. Voevodin, V. N. Balbyshev, M. Khobaib and M. S. Donley, *Progress in Organic Coatings*, 47 (2003) 416
17. Z .Szklarska-Smialowska and R. W. Staehle, J. Electrochem. Soc., 121 (1974) 1146
18. G. Adrian and A. Bittner, *Journal of Coating Technology*, 58 (1986) 59